Vol. 79: 137–147, 2017
https://doi.org/10.3354/ame01820

AQUATIC MICROBIAL ECOLOGY
Aquat Microb Ecol

Published online May 12

Elevated CO_2 and associated seawater chemistry do not benefit a model diatom grown with increased availability of light

Nana Liu[1], John Beardall[1,2], Kunshan Gao[1,*]

[1]State Key Laboratory of Marine Environmental Science/College of Ocean and Earth Sciences, Xiamen University, Xiang-An campus, Xiamen 361005, PR China

[2]School of Biological Sciences, Monash University, Clayton 3800, Victoria, Australia

ABSTRACT: Elevated CO_2 is leading to a decrease in pH in marine environments (ocean acidification [OA]), altering marine carbonate chemistry. OA can influence the metabolism of many marine organisms; however, no consensus has been reached on its effects on algal photosynthetic carbon fixation and primary production. Here, we found that when the diatom *Phaeodactylum tricornutum* was grown under different pCO_2 levels, it showed different responses to elevated pCO_2 levels under growth-limiting (20 µmol photons m^{-2} s^{-1}, LL) compared with growth-saturating (200 µmol photons m^{-2} s^{-1}, HL) light levels. With pCO_2 increased up to 950 µatm, growth rates and primary productivity increased, but in the HL cells, these parameters decreased significantly at higher concentrations up to 5000 µatm, while no difference in growth was observed with pCO_2 for the LL cells. Elevated CO_2 concentrations reduced the size of the intracellular dissolved inorganic carbon (DIC) pool by 81% and 60% under the LL and HL levels, respectively, with the corresponding photosynthetic affinity for DIC decreasing by 48% and 55%. Little photoinhibition was observed across all treatments. These results suggest that the decreased growth rates under higher CO_2 levels in the HL cells were most likely due to acid stress. Low energy demand of growth and energy saving from the down-regulation of the CO_2 concentrating mechanisms (CCM) minimized the effects of acid stress on the growth of the LL cells. These findings imply that OA treatment, except for down-regulating CCM, caused stress on the diatom, reflected in diminished C assimilation and growth rates.

KEY WORDS: Ocean acidification · Intracellular DIC · Photosynthesis

INTRODUCTION

Driven by human activity, such as fossil fuel combustion and deforestation, the atmospheric partial pressure of CO_2 (pCO_2) has increased by nearly 40% since pre-industrial times (IPCC 2007). As the principal sink, the ocean has absorbed approximately 30% (IPCC 2014) of anthropogenically derived CO_2, causing ocean acidification (OA), with the ocean pH predicted to decrease by 0.3 to 0.4 units by the end of this century (Sabine et al. 2004, Mikaloff Fletcher et al. 2006, Beardall et al. 2009). In addition to global OA driven by anthropogenic CO_2 release (IGBP 2013), additional acidification events occur on a regional scale as a consequence of localized upwelling of cold, CO_2-rich water and of volcanic CO_2 vents such as those in the Mediterranean and Circum-Pacific volcanic arcs, where pH values can be as low as 6.57, approximately equivalent to a pCO_2 of 20753 µatm (Sano & Williams 1996, Hall-Spencer et al. 2008, Dias et al. 2010). Such intensified CO_2 enrichment and altered seawater carbonate chemistry have consequences for primary productivity and growth of various organisms (Häder et al. 2015). Decreases in seawater pH can affect the intracellular acid-base balance of organisms, leading to enhanced energy

*Corresponding author: ksgao@xmu.edu.cn

demand; consequently, the membrane electrochemical potential and enzyme activity may be indirectly affected (Madshus 1988, Kramer et al. 2003, Milligan et al. 2009). Cytoplasmic pH is relatively constant under changes of external pH (Smith & Raven 1979), though intracellular pH in a coccolithophore was slightly reduced by the external pH drop associated with OA treatment (Nimer et al. 1994).

However, because of the paucity of knowledge on the physiological effects of OA, it is still controversial whether future carbon sequestration via the function of phytoplankton will increase or decline due to the progressive OA resulting from the accumulation of CO_2 in the atmosphere and its continuous dissolution into oceans. Importantly, while elevated pCO_2 levels can down-regulate CO_2 concentrating mechanisms (CCM) in the many aquatic photosynthetic organisms tested, it is still unclear if lowered energy costs due to down-regulation of CCM activity (Deng et al. 2003, Hopkinson et al. 2011) can compensate for the additional stresses associated with a pH drop, particularly at lower light levels encountered at depths in the oceans (Madshus 1988, Beardall et al. 1998, Kramer et al. 2003, Milligan et al. 2009, Raven et al. 2014). Acclimation to low-photon flux may also lead to a reduced capacity to employ a CCM which down-regulates under sub-saturating irradiance (Beardall & Giordano 2002, Yang & Gao 2012), leading to an increase in cells' reliance on CO_2 diffusion (Fu & Han 2010, Hepburn et al. 2011). Under high irradiance, CCM is expressed under ambient pCO_2 levels but is down-regulated with increasing pCO_2 (Wu et al. 2010, Li et al. 2014). There are documented data showing that elevated pCO_2 stimulated growth of some diatoms grown under low light (Gao et al. 2012, Li & Campbell 2013), but adverse effects on photosynthetic performance and growth (see Gao & Campbell 2014 and literature therein) have also been reported. In addition, whether intracellular inorganic carbon pools in diatoms would increase or decrease under OA conditions has not been experimentally demonstrated.

Phaeodactylum tricornutum, widely distributed around the world, is universally known as a model diatom for studies. The completely sequenced genome (http://genome.jgi-psf.org/Phatr2/Phatr2.home.html) permits follow-up studies depending on genetic information. Here, we grew the marine diatom *P. tricornutum* under growth-limiting (LL) and growth-saturating (HL) light levels at 4 different pCO_2 levels from 400 to 5000 µatm and showed that OA at the level expected by the end of the century (pH 7.8, 1000 µatm pCO_2) caused a slight increase in carbon assimilation and growth. However, more intense acidification at higher levels of pCO_2 partially reduced activity of CCM and internal inorganic carbon pools and had a negative impact on cells' carbon fixation capacity. We also showed that the harmful impacts of OA were enhanced at HL, but much reduced at the LL level, under energy-limited conditions.

MATERIALS AND METHODS

Organism model and algal culture conditions

A culture of *Phaeodactylum tricornutum* strain CCMA 106 was obtained from the Center for Collections of Marine Bacteria and Phytoplankton (CCMBP) of the State Key Laboratory of Marine Environmental Science (Xiamen University). This strain was originally isolated from the South China Sea. It was grown in artificial seawater with Aquil (Morel et al. 1979) medium enrichment. We diluted the cultures semi-continuously every 24 h and aerated them at 350 ml min^{-1} with air containing target CO_2 concentrations of 400, 950, 2250 or 5000 µatm. The pCO_2 levels were obtained by a CO_2 enricher (CE-100B, Wuhan Ruihua Instrument & Equipment, China), and the target pCO_2 levels were checked with a carbon dioxide sensor (GM70, Vaisala, Finland). Elevated pCO_2 levels are the driver for acidification of seawater, and the procedure here follows standard best practice for OA research (Riebesell et al. 2010). Cells at densities between 2.5×10^4 and 1.8×10^5 ml^{-1} were grown under a 12 h light:12 h dark photoperiod at 200 or 20 µmol photons m^{-2} s^{-1} and 20°C. The compensation point for growth of *P. tricornutum* has been reported to be 0.5 µmol photons m^{-2} s^{-1} (Geider et al. 1986). Experiments were initiated after the alga had acclimated to each treatment condition for at least 8 generations and only after a constant growth rate had been recorded for 3 further consecutive sampling periods.

Carbonate system chemistry in cultures

The pH was measured 3 to 5 times prior to dilution for each treatment with a pH meter (Benchtop pH510; OAKTON) calibrated with the National Bureau of Standards buffer solution (Hanna). With the known values of pH, salinity, nutrients, temperature, and pCO_2, other associated parameters of the carbonate chemistry of the cultures were estimated using the program CO_2SYS (Lewis & Wallace 1998). The equilibrium constants (K_1 and K_2) for carbonic

acid (Roy et al. 1993) and boric acid (Dickson 1990) dissociation were used for all calculations.

Growth rate and chlorophyll measurements

We measured cell numbers with a Coulter Counter (Z-2, Beckman) before and after culture dilution, and growth rate was calculated according to the following equation: $\mu = (\ln N_1 - \ln N_0)/(t_1 - t_0)$, where N_0 and N_1 refer to the cell concentration immediately after the dilution and before the next dilution, respectively, and $t_1 - t_0$ is the time (days, 1 d in this experiment) between the dilutions. For chlorophyll *a* (chl *a*) determination, 150 ml samples under steady state growth conditions were filtered onto a Whatman GF/F filter (25 mm), extracted in 5 ml 100% methanol overnight at 4°C, and then centrifuged at 5000 × *g* for 10 min. The absorbance of the supernatant was scanned from 250 to 800 nm with a scanning spectrophotometer (DU 800, Beckman Coulter). The cellular chl *a* and carotenoid content were calculated according to the equations of Ritchie (2006) and Strickland & Parsons (1968), respectively.

Photosynthetic carbon fixation

Cells were incubated under the growth light and pCO_2 levels (initial cell concentration was 5000 cell ml^{-1}; fresh medium was aerated with target gas before incubation) with 5 µCi (0.185 MBq) $NaH^{14}CO_3$ (ICN Radiochemicals, Irvine, CA, USA) for 12 h (full light period only) or 24 h (light and the following dark period), respectively, and samples were filtered and collected every 12 h. The samples were then exposed to fuming HCl overnight and dried over the following 6 h, as previously reported (Gao et al. 2007). The ^{14}C assimilated into organic matter was counted using a liquid scintillation counter (Tri-Carb 2800TR, Perkin-Elmer, Waltham, USA). The carbon fixation rate was normalized to the initial cell concentration.

The relationship between photosynthesis and dissolved inorganic carbon (P vs. C curves) for *P. tricornutum* was measured at 20°C with 50 mM HEPES to maintain the pH at 8.0 under a photosynthesis-saturating light level of 400 µmol photons m^{-2} s^{-1} (Geider et al. 1985, Zou & Gao 2014) at different levels of DIC.

Determination of intracellular inorganic carbon

The intracellular inorganic carbon pools were measured using the silicone oil centrifugation technique (Badger et al. 1980, Johnston & Raven 1996, Tortell et al. 2000). Inorganic C-depleted cell suspensions (buffered with 50 mM HEPES) were firstly prepared and placed in the dark. Prior to addition to centrifuge tubes that contained 100 µl of 2.5 N NaOH in 10% methanol (bottom layer) and 200 µl silicone oil (middle layer), 200 µl aliquots of inorganic C-depleted cell suspensions were pre-illuminated for 2 min under 600 µmol photons m^{-2} s^{-1} (Ratti et al. 2007). Subsequently, as soon as 100 µl of $NaH^{14}CO_3$ stock solution (5 µCi, 0.185 MBq) was injected into the individual tube, the cell suspensions were mixed thoroughly and incubated at the same light intensity for 10 s. Suspensions were then centrifuged at 18 000 × *g* for 40 s to terminate the incubations, separating the cells from the ^{14}C solution by passage through the middle (oil) layer into the NaOH-methanol solution. We then froze the tubes immediately with liquid nitrogen, followed by removal of the cell pellets and their resuspension into scintillation vials containing 1 ml of 0.5 N NaOH. After mixing thoroughly, 0.5 ml of the resuspended pellet solution was transferred into another fresh vial, thereby obtaining 2 subsamples. One of these was used for estimation of organic C by acidification with 0.5 ml of 2 N HCl and leaving the contents to degas unassimilated $^{14}HCO_3^-$ for at least 12 h. The second sample was left in 0.5 N NaOH and provided a count of inorganic plus organic ^{14}C. The amount of radioactivity was determined in each sample by liquid scintillation counting. The amount of inorganic C inside the cells is given by the difference between total (inorganic + organic) and acid-stable (organic) ^{14}C in the cell pellets.

Intracellular inorganic C concentrations were calculated by normalizing the amount of carbon to intracellular volume (mannitol-impermeable), which was measured by incubating samples for 30 to 40 s with ^3H_2O and ^{14}C-mannitol and centrifugation as described above. These labelled compounds provide an estimation of total biovolume (^3H_2O) and extracellular H_2O space (D-[1-^{14}C]-mannitol) (Badger et al. 1980, Ratti et al. 2007).

We carried out the experiment for the determination of intracellular volume and extracellular water under low light and 20°C conditions.

Photochemical parameters

To estimate the photochemical responses of the cells to changes in pCO_2 and light intensities, the maximum photochemical quantum yield (F_v/F_m), effective quantum yield in the light (Φ_{PSII}) and rapid

light curves (RLCs) were measured using a Xenon-Pulse Amplitude Modulated fluorometer (XE-PAM, Walz, Germany). F_v is the maximum wavelength of the variable fluorescence when all the non-photochemical processes are minimum under dark adaptation state; F_m is the maximum fluorescence when all the reaction centers of photosynthetic system II are closed and all the non-photochemical processes are minimum under dark adaptation state. RLCs determined the relative electron transport rates (rETR) when cells were exposed to 8 different and increasing light levels (0, 76, 156, 226, 337, 533, 781, 1077 and 1593 µmol photons m^{-2} s^{-1}), with a 15 s duration of exposure to each level separated by a 0.8 s saturating pulse (3000 µmol photons m^{-2} s^{-1}).

At the middle of the photoperiod, samples were taken and kept in the dark for 15 min prior to determination of F_v/F_m and RLC. Φ_{PSII} was measured at the actinic light levels close to the growth light intensities 76 (a growth-limiting light level) and 226 µmol photons m^{-2} s^{-1} (a growth-saturating light level, Gao et al. 2012). rETR at each light level was calculated as rETR = $\Phi_{PSII} \times 0.5 \times$ PPFD, where Φ_{PSII} is the effective photochemical quantum yield of PSII, and the factor 0.5 accounts for approximately 50% of all the absorbed energy being allocated to PSII. The rETR data were fitted to light intensity with the equation of Eilers & Peeters (1988): $y = x/(ax^2 + bx + c)$, where a, b, c are estimated parameters, x is photon flux density, and y is the rETR value. Maximal relative electron transport rate ($rETR_{max}$) and light saturation point (E_k) were then calculated according to the equations: $rETR_{max} = 1/[b + 2(ac)^{1/2}]$, $E_k = c/[b + 2(ac)^{1/2}]$, and α (light use efficiency) was determined as $\alpha = 1/c$.

Data analysis

One-way ANOVA and Tukey tests as well as 2-sample *t*-tests were used to establish differences and interactions among these treatments. The significance level was set at $p < 0.05$.

RESULTS

Carbonate system

The pH levels in the different treatments varied from 8.17 (± 0.01) to 7.19 (± 0.01), being significantly different ($p < 0.01$) across pCO_2 levels but not across low- and high-light acclimations under the same pCO_2 level ($p > 0.05$) (see Table S1 in the Supplement at www.int-res.com/articles/suppl/a079p137_supp.pdf). With increased pCO_2 levels, DIC changed from 1918.91 ± 45.87 (SD) to 2547.50 ± 16.95 µmol kg^{-1}, though the changes in total alkalinity (TA) across all treatments were <6%. During the process of pCO_2 increasing from 400 to 5000 µatm, HCO_3^- and $CO_{2(aq)}$ concentrations increased by 36.67% and 115%, respectively, and CO_3^{2-} concentration decreased approximately 7-fold.

Growth and chlorophyll responses

Light intensity had a significant effect on the growth of *Phaeodactylum tricornutum*, such that the growth rates of the HL cultured cells were more than twice those at low light ($p < 0.01$). For the HL cultured cells, the peak value of growth rate was recorded at 950 µatm pCO_2 (Fig. 1). Compared to the 400 µatm pCO_2 treatment, a significant difference ($p = 0.004$) was detected. When pCO_2 was increased further (to 5000 µatm), we observed a considerable decline in the growth of the HL grown cells. Additionally, the variation in growth rate with pCO_2 of the LL cultured cells was relatively minor compared with that of the HL incubated algae. Similarly, compared to the 400 µatm pCO_2 treatment, small but statistically significant enhancements of growth were observed for the LL cells grown under the 950 µatm ($p = 0.045$) and 2250 µatm ($p = 0.018$) conditions. However, the

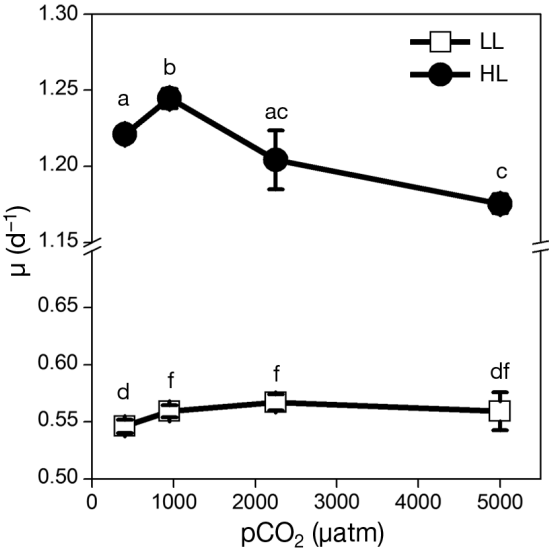

Fig. 1. Growth rates of (µ) *Phaeodactylum tricornutum* under a matrix of pCO_2 and light. Different letters indicate significant differences among all treatments including different pCO_2 and light conditions. Data are means ± SD, n = 3. HL: high light, 200 µmol photons m^{-2} s^{-1}; LL: low light, 20 µmol photons m^{-2} s^{-1}

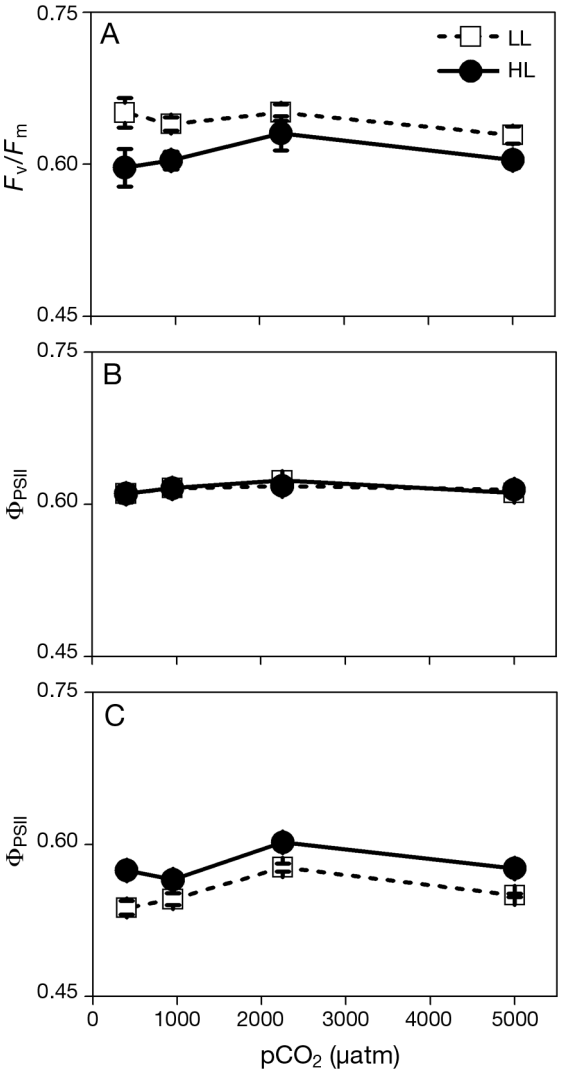

Fig. 2. (A) Maximum photochemical quantum yield (F_v/F_m) measured after dark incubation. (B) Effective quantum yield in the light (Φ_{PSII}) assessed under 76 µmol photons m^{-2} s^{-1}, limiting light for growth. (C) Φ_{PSII} assessed under 226 µmol photons m^{-2} s^{-1}, saturation light for growth. LL and HL represent cells cultured under 20 and 200 µmol photons m^{-2} s^{-1} for at least 8 generations, respectively. Data are means ± SD, n = 3

LL acclimated cells' growth rate showed almost no change when the pCO_2 increased to 5000 µatm (Fig. 1). Overall, the response of growth rate to CO_2 was much less in the LL acclimated cells than in the HL treatments.

Analysing across all the pCO_2 levels, there was a significant difference in chl *a* content between the 2 light intensity treatments ($p < 0.01$; see Table S2 in the Supplement), with marked enhancements, varying from 34.30% to 51.4%, under low-light conditions compared with high light. The chl *a* content was, however, not significantly affected by pCO_2 levels. The carotenoid contents of cells were unaffected by pCO_2 or light levels. The cells grown under high light showed higher ratios of carotenoids to chl *a*, and a significant difference in this ratio was observed between the 2 light levels. For the high light level, compared to the low pCO_2 treatments, this ratio decreased markedly for algae cultured at high pCO_2 levels, including 2250 and 5000 µatm ($p < 0.001$; Table S2).

Photochemical responses

F_v/F_m and Φ_{PSII} at 76 and 226 µmol photons m^{-2} s^{-1} are shown in Fig. 2. The variation of pCO_2 levels had no significant influence on the maximal quantum yield and effective quantum yield. E_k and $rETR_{max}$ of *P. tricornutum* increased with light and pCO_2 levels (Fig. 3A,B). However, regardless of the different light treatments, the change in the light use efficiency α with pCO_2 was small at LL and absent in HL cultures (Fig. 3C), although absolute values of α were 1.20- to 1.34-fold higher in LL cultures than in those of HL cells (Fig. 3D).

Carbon fixation

The net carbon fixation rates at the growth light levels over 12 h or 24 h are shown in Fig. 4. The carbon fixation rate for the HL acclimated cells was 2.1- to 3.9-fold that of the LL acclimated cells. Across all the light and incubation period treatments, carbon fixation varied in the same way with different pCO_2 treatments. As shown in Fig. 4, the same trend of an initial slight increase to 950 µatm then a decrease in fixation rates at the highest pCO_2 was observed. However, except for the HL and 5000 µatm acclimated cells, no significant difference of 24 h carbon fixation rates with pCO_2 were found due to a large variance in the data (Fig. 4B). As shown in Fig. 4A, considerable changes in 12 h carbon fixation rate were observed for both light intensity treatments, but with a similar trend of a slight increase from 400 to 950 µatm and then a decrease at higher CO_2 levels.

Affinity of cells for dissolved inorganic carbon

The conventional measure of affinity of cells for inorganic carbon is $K_{0.5}$; however, this parameter was strongly affected by the significant decrease in maximal rates of carbon fixation and truncation of P vs.

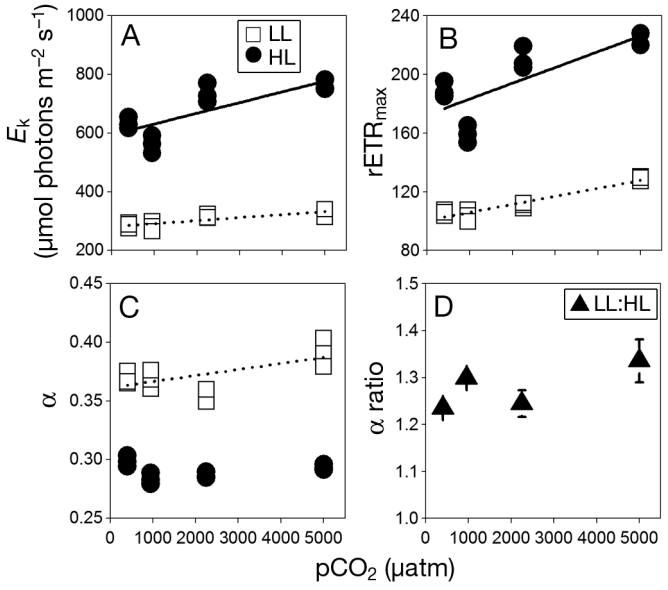

Fig. 3. Fluorescence parameters calculated from the rapid light curve relative to pCO_2 levels under different light intensities. (A) Light saturation point (E_k), µmol photons m^{-2} s^{-1}; low light (LL, 20 µmol photons m^{-2} s^{-1}): R^2 = 0.65 ($p < 0.01$); high light (HL, 200 µmol photons m^{-2} s^{-1}), R^2 = 0.58 ($p < 0.01$). (B) Maximal relative electron transport rate ($rETR_{max}$); LL: R^2 = 0.90 ($p < 0.01$); HL: R^2 = 0.55 ($p < 0.01$). (C) Light use efficiency (α); LL: R^2 = 0.36 ($p < 0.05$); HL: showed very low R^2. (D) The ratio of α for LL acclimated cells to that of HL acclimated cells showed very low R^2. The solid line and short dotted line represent the best fit for the HL and LL cultured cells, respectively. LL and HL represent cells cultured under 20 and 200 µmol photons m^{-2} s^{-1} for at least 8 generations, respectively. Data are means ± SD, n = 3. One data point, for α at 2250 µatm at low light, was an evident outlier and was deleted from the analysis

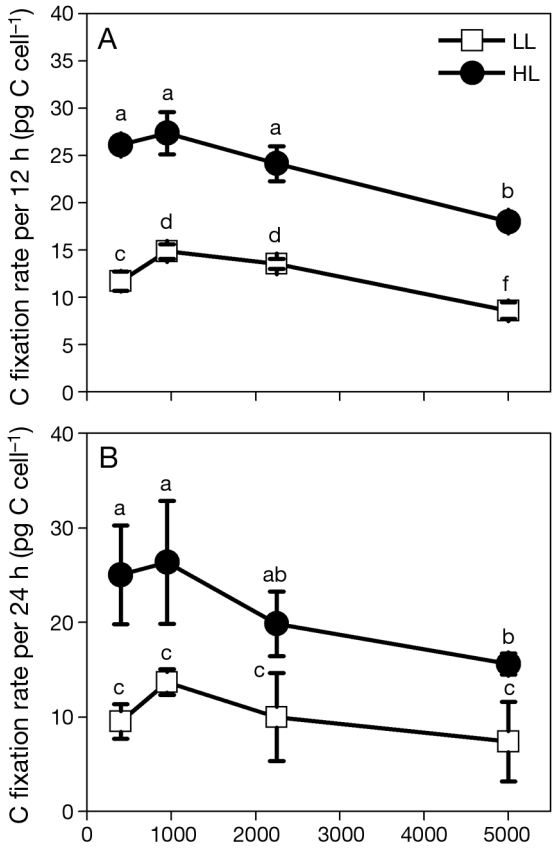

Fig. 4. Carbon fixation per cell during (A) daytime (12 h) and (B) on a daily basis (24 h) in *Phaeodactylum tricornutum* cells grown under different levels of pCO_2 and light (LL: 20 µmol photons m^{-2} s^{-1}; HL: 200 µmol photons m^{-2} s^{-1}). Different letters above the symbols present significant differences among the treatments. Data are the means ± SD, n = 3 (triplicate independent cultures)

DIC curves in cells shown in Fig. S1 (in the Supplement), and so is not used here (data shown in Table S3 in the Supplement), though for the cells grown under HL, $K_{0.5}$ values increased significantly from 400 to 950 µatm then leveled off at higher CO_2 levels. Values of the slopes of carbon fixation vs. DIC (conductance) were higher in the cells grown under HL than in cells from LL conditions, but in both HL and LL cells, values were approximately stable until pCO_2 for growth exceeded 2250 µatm (Fig. 5A). However, in comparison to the 400 µatm, the conductance declined considerably at 5000 µatm, by 48% and 55% for the LL and HL treatments, respectively.

Maximal values of V_{max} were recorded at 950 and 2250 µatm for the LL and HL cultures, respectively (Fig. 5B). V_{max} of cells grown under 5000 µatm was significantly lower for both light treatments, compared to the maximum values. When rates of C fixation at the growth CO_2 concentrations are calculated from the data shown in Fig. S1, a peak in C fixation rate is found at 2250 µatm with rates decreasing at higher CO_2 concentration (Fig. S3).

The silicone oil centrifugation data showed that the intracellular volume was about 60 $µm^3$ with no significant difference among the treatments. However, as shown in Fig. 6A, cells cultured at 5000 µatm pCO_2 had much lower (60.1 to 80.6%) intracellular inorganic carbon concentration than those grown at 400 µatm pCO_2. In the cells grown under 5000 µatm pCO_2, the internal pool was 603 and 1639 µmol l^{-1} under the LL and HL conditions respectively, representing about a 5.3-fold drop (2603.5 ± 282.8 µmol l^{-1}) in the intracellular DIC pool for the LL cultures and a 2.5-fold decline (2473.2 ± 248.1 µmol l^{-1}) in the cells grown under HL compared to the cells acclimated to 400 µatm (Fig. 5A). The percentage decline of internal DIC concentration was also considerably ($p = 0.032$, *t*-test) impacted by different light treatments.

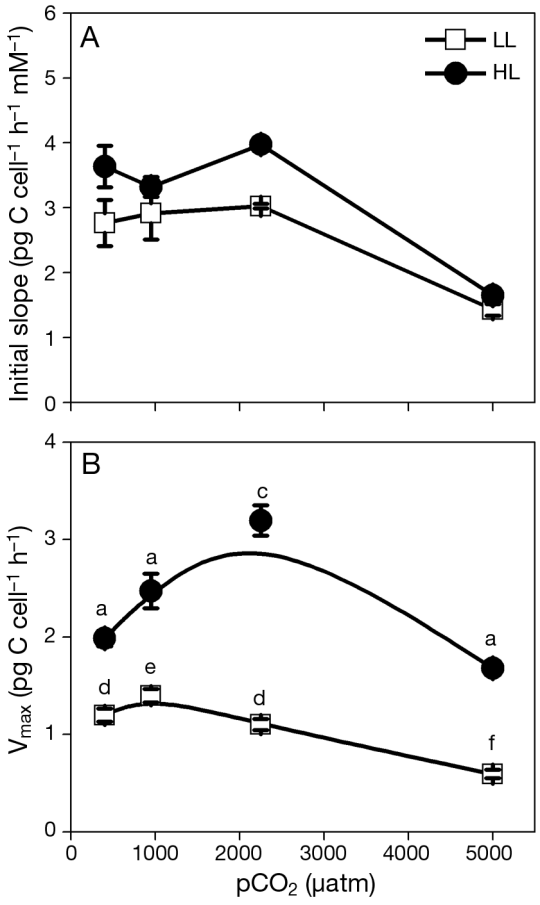

Fig. 5. Parameters derived from Fig. S1 are shown under a matrix of pCO_2 and light for *Phaeodactylum tricornutum*. (A) Initial slope (see Fig. S1) of photosynthesis vs. dissolved inorganic carbon (DIC, pg C cell^{-1} h^{-1} mM^{-1}); (B) DIC-saturated and light-saturated rates of photosynthesis, V_{max}, which was calculated according to the Michaelis-Menten function. Data are the means ± SD, n = 3. Different letters above the symbols indicate significant differences among the treatments, each of which was represented by triplicate cultures grown under low light (LL, 20 µmol photons m^{-2} s^{-1}) and high light (HL, 200 µmol photons m^{-2} s^{-1}) conditions

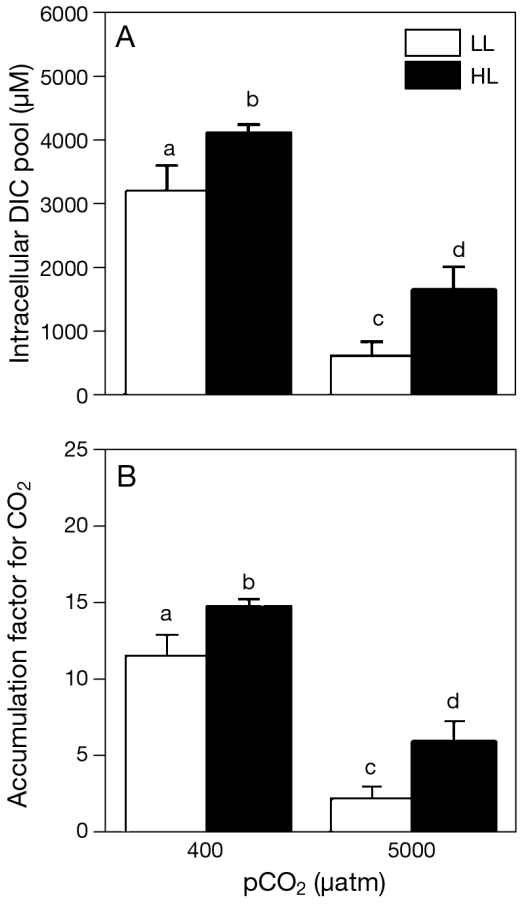

Fig. 6. Intracellular DIC pool and accumulation factor for CO_2 measured through silicone oil centrifugation experiments. (A) intracellular dissolved inorganic carbon (DIC) pools of *Phaeodactylum tricornutum* grown under 400 and 5000 µatm pCO_2 as well as the low light (LL, 20 µmol photons m^{-2} s^{-1}) and high light (HL, 200 µmol photons m^{-2} s^{-1}) levels; (B) accumulation factor for CO_2 for different treatments. Different letters above the columns indicate significant differences among the treatments, each of which was represented by triplicate cultures. Error bars = 1 SD

Since it is the increased availability of CO_2 at the active site of Rubisco (the pyrenoid, in species that have them; Beardall 1991, Beardall & Giordano 2002, Hopkinson et al. 2011) rather than overall cellular accumulation of DIC that determines CCM activity (but acknowledging that it is impossible to determine [DIC] and pH in specific cell organelles), we used a value for mean internal pH of 7.59 for microalgae cells (Burns & Beardall 1987, Raven 1990) and thus assessed the accumulation factors ($[CO_2]_{inside}$: $[CO_2]_{outside}$) based on the calculated average internal CO_2 levels. These factors were estimated to be 14.7 and 11.5 for cells grown at 400 µatm under HL and LL conditions, respectively (Fig. 6B). At 5000 µatm pCO_2, they dropped to 5.9 at HL and to 2.2 (Fig. 6B) at LL. In short, therefore, the cells grown under LL and high CO_2 had the smallest intracellular DIC pools: about 5.8-fold smaller than that in the cells grown under the HL and low CO_2 levels.

DISCUSSION

Acid stress under high CO_2?

Under the high light level for growth, elevated pCO_2 at the concentration expected by the end of the century caused a small, but statistically significant, rise in growth rates; pCO_2 at the higher concentra-

tions, representing what might be found in upwellings and volcanic seeps, caused a decline in growth. However, the decline in growth rate at higher pCO_2 levels was not the case at low light, where growth was almost independent of pCO_2. The reasons contributing to this phenomenon, observed under HL conditions, could be twofold: (1) photoinhibition and (2) acid stress.

In relation to photoinhibition, cells grown under both HL and LL conditions showed no effect on maximal quantum yield of PSII with increased pCO_2 and exhibited increases in parameters such as E_k and $rETR_{max}$ at higher CO_2 levels. Similar responses to elevated pCO_2 have also been shown for the cyanobacterium *Cylindrospermopsis* (Pierangelini et al. 2014), indicating that higher electron transport rates were achieved when higher pCO_2 was applied to the cells, and that photoinhibition, in terms of rETR at least, was not occurring under any of the treatments, though photorespiratory O_2 consumption has been reported to be enhanced by ~26% in the same species grown under 1000 µatm pCO_2 (Gao et al. 2012). This lack of photoinhibition was also demonstrated by the absence of significant non-photochemical quenching (NPQ) for the cells under all incubation conditions in this experiment (data not shown). Thus, photoinhibition is out of the question as a driver of the significantly decreased growth rates at high pCO_2, and acid stress might therefore be the cause. The effects of pCO_2 were stronger at saturating light intensity than under limiting light, except for the light harvesting efficiency (α), which was enhanced at low light but decreased with increased photosynthetic affinity for CO_2 (CCM activity) (Fig. S2). Meanwhile, these results demonstrate that OA did not stress the photochemical reactions of PSII, even under intense OA induced at 5000 µatm pCO_2.

Acid stress vs. downregulation of the CO_2 concentrating mechanisms

It is possible that the impact of acidification overwhelmed any performance-enhancing effects of increased pCO_2 and energy saving from down-regulation of the CCM, a feature previously suggested for a coccolithorphorid (Fukuda et al. 2014). When pH *in milieu* declines due to increased pCO_2, cells usually acclimate to maintain the normal operation of redox systems on the plasma membrane (Suffrian et al. 2011) and drive H^+ efflux to maintain a constant intracellular pH environment via proton pumps and/or operation of the H^+-translocating ATPase (Madshus 1988), a process that is energy demanding (Smith & Raven 1979, Suffrian et al. 2011). Extra H^+-efflux by H^+-ATPase leads to a more acidic local environment surrounding the cell, which could have impacts on the redox systems of the plasma membrane, associated with nutrient (iron, nitrate, etc.) uptake, through the influence on the activities of transmembrane and apoplastic-side plasma membrane enzymes (Jones & Morel 1988, Moog & Brüggemann 1994). While down-regulation of the CCM in diatoms can save energy involved in active inorganic carbon (Ci) acquisition (Hopkinson et al. 2011, Hennon et al. 2014), direct measurements of intracellular pCO_2 levels in these cells under OA have not previously been carried out. In the current work, we have demonstrated that the inorganic carbon pools within the diatom cells declined with elevated pCO_2 within the range expected from climate change and natural high CO_2 systems in the oceans.

As reflected in the initial slope of photosynthesis-dissolved inorganic carbon curves, which correlates with photosynthetic affinity for DIC (Beardall 1991, Johnston et al. 1992), CCM activity of the cells grown under HL and LL was significantly down-regulated with increasing pCO_2. The intracellular dissolved inorganic carbon pool, assessed with the silicone oil technique, distinctly decreased under the elevated CO_2 level, regardless of HL and LL conditions (there was a significant difference between the decline for the 2 light intensities, $p = 0.032$). The percentages of CCM down-regulation for the HL and LL cells were 60% and 81%, respectively, confirming that the down-regulation of the CCM under the high CO_2 conditions (400 µatm vs. 5000 µatm) was more pronounced under the LL treatment.

The mismatch between changes in the photosynthetic affinity of cells for DIC and differences in intracellular DIC pools could be explained by the localized DIC hypothesis (Raven 1997), whereby cells could accumulate CO_2 around the site of Rubisco activity without the necessity for a high overall intracellular DIC (Matsuda et al. 2011, Hopkinson 2014). Therefore, the relatively lower intracellular DIC pool for the cells grown under 5000 µatm pCO_2 may not reflect the true activity of steady state CCM for *P. tricornutum*. Associated with the combined effects of both increased harm from the pH decline and benefits from increased DIC availability at elevated pCO_2, we expected that there may be a point beyond which the CCM is not further down-regulated, though the point cannot be demonstrated well from our data. On the basis of the changes in initial slope of P vs. DIC curves within our experiments, we

expect that the point for this balance could be above 5000 µatm and vary under different light treatments. Additionally, the balance point may be quite different for different DIC utilization mechanisms that are used by other algae (Aizawa & Miyachi 1986, Shiraiwa 2003, Tsuji et al. 2009).

In addition, although no impact on light harvesting efficiency (α) from increased CO_2 was observed for the HL cultured cells, that for the LL grown cells was positively related to the increasing pCO_2 (Fig. 3C). These observations may be due to the energetic limitation on the capacity of the cells grown under LL to utilize HCO_3^- by active transport and to develop CCM, thus enhancing their reliance on CO_2 diffusion (Hepburn et al. 2011, Gao & Campbell 2014). However, relatively highly expressed CCM was employed by the cells grown under HL. Furthermore, the growth rate and carbon fixation rate as well as relative electron transport were much higher for the HL cultured cells, which thus needed more DIC to achieve their growth rates compared to the ones grown under LL. As a result, the energy saved from the down-regulation of CCM activity may be used by the LL cultured cells to better deal with the pH decline as the pCO_2 increased in comparison with the HL cells (Raven et al. 2000, Li & Campbell 2013, Wu et al. 2010). This is supported by Fig. S2, which shows that α was negatively correlated with the initial slope of P vs. DIC curves at LL, but not in HL cultures, i.e. lower CCM activity was associated with greater efficiency of light harvesting. The major energy expenditure on the CCM is in the transport of DIC into the chloroplast (1 ATP per HCO_3^- molecule; Raven et al. 2000, Hopkinson et al. 2011) with 0.5 ATP for HCO_3^- transported across the external membrane of the cell. A 50% reduction in CCM capacity in cells grown at 5000 µatm CO_2 would thus save 0.75 ATP per CO_2 delivered, with the suppression of the photosynthetic carbon oxidation cycle by elevated CO_2 at the active site providing additional energy savings. Energy costs of pH regulation are complex, depending on a range of factors, including nutrient source and mechanism of pH homeostasis (Smith & Raven 1979). The influence of increased environmental H^+ concentration on the cell is not only related to pumping out the extra H^+ from the cells but also involves other complex cellular activities, so the energy costs associated with the decreased external pH cannot be calculated easily. Growth rate and carbon fixation rate may be more reliable metrics for demonstrating the pH effects.

Therefore, the decreased growth rates under higher pCO_2 levels in the HL cells were most likely attributable to acid stress. Compared to the large requirement for DIC acquisition by the HL cultured alga, the CO_2-diffusion-dependent cells grown under LL with little CCM activity must have benefited more from the increased $CO_{2(aq)}$. Our data demonstrate that seawater acidification, whether global due to anthropogenic forcings or regional due to coastal upwelling or areas of CO_2 seeps, will influence the physiology of diatoms, as exemplified by *P. tricornutum*. The down-regulation of CCM operation, leading to energy savings, partially overcame the negative impact of exacerbated acidity resulting from very high pCO_2. When we consider the impacts of regional acidification, the light available at different depths of water is likely to play an important role in regulating the physiological performance of phytoplankton, and interactions between CO_2 and light levels will be critical in this situation. Clearly, the responses shown here for *P. tricornutum* need to be investigated in a wider range of ecologically relevant species before any broad conclusions can be reached.

Acknowledgements. We are grateful for the help of S. Y. Tong during the experiments. We also thank Y. P. Wu, J. T. Xu and Y. H. Li for experimental advice. This study was supported by the National Natural Science Foundation (NSFC, No. 41430967; 41120164007), Joint project of the NSFC and Shandong province (Grant No. U1406403), Strategic Priority Research Program of the Chinese Academy of Sciences (Grant No. XDA11020302) and the State Oceanic Administration (SOA, GASI-03-01-02-04). J.B.'s work on climate change effects on algae has been funded by the Australian Research Council, and his visit to Xiamen was supported by a '111' project from the Ministry of Education. The authors have no conflicts of interest to declare.

LITERATURE CITED

Aizawa K, Miyachi S (1986) Carbonic anhydrase and CO_2 concentrating mechanism in microalgae and cyanobacteria. FEMS Microbiol Rev 39:215–233

Badger MR, Kaplan A, Berry JA (1980) Internal inorganic carbon pool of *Chlamydomonas reinhardtii*. Plant Physiol 66:407–413

Beardall J (1991) Effects of photon flux density on the 'CO_2-concentrating mechanism' of the cyanobacterium *Anabaena variabilis*. J Plankton Res 13:133–141

Beardall J, Giordano M (2002) Ecological implications of microalgal and cyanobacterial CCMs and their regulation. Funct Plant Biol 29:335–347

Beardall J, Johnston A, Raven JA (1998) Environmental regulation of CO_2-concentrating mechanisms in microalgae. Can J Bot 76:1010–1017

Beardall J, Stojkovic S, Larsen S (2009) Living in a high CO_2 world: impacts of global climate change on marine phytoplankton. Plant Ecol Divers 2:191–205

Burns BD, Beardall J (1987) Utilization of inorganic carbon by marine microalgae. J Exp Mar Biol Ecol 107:75–86

Deng Y, Ye J, Mi H (2003) Effects of low CO_2 on NAD (P) H dehydrogenase, a mediator of cyclic electron transport around photosystem I in the cyanobacterium *Synechocystis* PCC6803. Plant Cell Physiol 44:534–540

Dias B, Hart M, Smart C, Hall-Spencer J (2010) Modern seawater acidification: the response of foraminifera to high-CO_2 conditions in the Mediterranean Sea. J Geol Soc London 167:843–846

Dickson AG (1990) Standard potential of the reaction: AgCl (s) + $12H_2$ (g) = Ag (s) + HCl (aq), and and the standard acidity constant of the ion HSO_4^- in synthetic sea water from 273.15 to 318.15 K. J Chem Thermodyn 22: 113–127

Eilers PHC, Peeters JCH (1988) A model for the relationship between light intensity and the rate of photosynthesis in phytoplankton. Ecol Model 42:199–215

Fu X, Han B (2010) Response of cyanobacterial carbon concentrating system to light intensity: a simulated analysis. Chin J Oceanology Limnol 28:478–488

Fukuda SY, Suzuki Y, Shiraiwa Y (2014) Difference in physiological responses of growth, photosynthesis and calcification of the coccolithophore *Emiliania huxleyi* to acidification by acid and CO_2 enrichment. Photosynth Res 121:299–309

Gao KS, Campbell DA (2014) Photophysiological responses of marine diatoms to elevated CO_2 and decreased pH: a review. Funct Plant Biol 41:449–459

Gao KS, Wu YP, Li G, Wu HY, Villafañe VE, Helbling EW (2007) Solar UV radiation drives CO_2 fixation in marine phytoplankton: a double-edged sword. Plant Physiol 144: 54–59

Gao KS, Xu JT, Gao G, Li YH and others (2012) Rising CO_2 and increased light exposure synergistically reduce marine primary productivity. Nat Clim Chang 2: 519–523

Geider RJ, Osborne BA, Raven JA (1985) Light dependence of growth and photosynthesis in *Phaeodactylum tricornutum.* J Phycol 21:609–619

Geider RJ, Osborne BA, Raven JA (1986) Growth, photosynthesis and maintenance metabolic cost in the diatom *Phaeodactylum tricornutum* at very low light levels. J Phycol 22:39–48

Häder DP, Williamson CE, Wangberg SA, Rautio M and others (2015) Effects of UV radiation on aquatic ecosystems and interactions with other environmental factors. Photochem Photobiol Sci 14:108–126

Hall-Spencer JM, Rodolfo-Metalpa R, Martin S, Ransome E and others (2008) Volcanic carbon dioxide vents show ecosystem effects of ocean acidification. Nature 454: 96–99

Hennon GM, Quay P, Morales RL, Swanson LM, Virginia AE (2014) Acclimation conditions modify physiological response of the diatom *Thalassiosira pseudonana* to elevated CO_2 concentrations in a nitrate-limited chemostat. J Phycol 50:243–253

Hepburn C, Pritchard D, Cornwall C, McLeod RJ and others (2011) Diversity of carbon use strategies in a kelp forest community: implications for a high CO_2 ocean. Glob Change Biol 17:2488–2497

Hopkinson BM (2014) A chloroplast pump model for the CO_2 concentrating mechanism in the diatom *Phaeodactylum tricornutum.* Photosynth Res 121:223–233

Hopkinson BM, Dupont CL, Allen AE, Morel FMM (2011) Efficiency of the CO_2-concentrating mechanism of diatoms. Proc Natl Acad Sci USA 108:3830–3837

IGBP, IOC, SCOR (2013) Ocean Acidification Summary for Policy makers. 3rd Symposium on the Ocean in a High-CO_2 World. International Geosphere-Biosphere Programme, Sep 2012, Stockholm

IPCC (Intergovernmental Panel on Climate Change (2007) Climate Change 2007: The physical science Basis. Contribution of Working Group I to the Fourth Assessment Report of the Intergovernmental Panel on Climate Change. In: Solomon S, Qin D, Manning M, Chen Z and others (eds) Cambridge University Press, Cambridge and New York, NY

IPCC (Intergovernmental Panel on Climate Change) (2014) Climate Change 2014: synthesis report. Contribution of Working Groups I, II and III to the Fifth Assessment Report of the Intergovernmental Panel on Climate Change. In: Core Writing Team, Pachauri R, Meyer L (eds). IPCC, Geneva

Johnston AM, Raven JA (1996) Inorganic carbon accumulation by the marine diatom *Phaeodactylum tricornutum.* Eur J Phycol 31:285–290

Johnston AM, Maberly S, Raven JA (1992) The acquisition of inorganic carbon by four red macroalgae. Oecologia 92:317–326

Jones GJ, Morel FMM (1988) Plasmalemma redox activity in the diatom *Thalassiosira.* Plant Physiol 87:143–147

Kramer DM, Cruz JA, Kanazawa A (2003) Balancing the central roles of the thylakoid proton gradient. Trends Plant Sci 8:27–32

Lewis E, Wallace D (1998) Program developed for CO_2 system calculations, ORNL/CDIAC-105. US Department of Energy, Carbon Dioxide Information Analysis Center, Oak Ridge National Laboratory, Oak Ridge, TN

Li G, Campbell DA (2013) Rising CO_2 interacts with growth light and growth rate to alter photosystem II photoinactivation of the coastal diatom *Thalassiosira pseudonana.* PLOS ONE 8:e55562

Li Y, Xu JT, Gao KS (2014) Light-modulated responses of growth and photosynthetic performance to ocean acidification in the model diatom *Phaeodactylum tricornutum.* PLOS ONE 9:e96173

Madshus IH (1988) Regulation of intracellular pH in eukaryotic cells. Biochem J 250:1–8

Matsuda Y, Nakajima K, Tachibana M (2011) Recent progresses on the genetic basis of the regulation of CO_2 acquisition systems in response to CO_2 concentration. Photosynth Res 109:191–203

Mikaloff Fletcher SE, Gruber N, Jacobson AR, Doney SC and others (2006) Inverse estimates of anthropogenic CO_2 uptake, transport, and storage by the ocean. Global Biogeochem Cycles 20:GB2002

Milligan AJ, Mioni CE, Morel FM (2009) Response of cell surface pH to pCO_2 and iron limitation in the marine diatom *Thalassiosira weissflogii.* Mar Chem 114:31–36

Moog PR, Brüggemann W (1994) Iron reductase systems on the plant plasma membrane — a review. Plant Soil 165: 241–260

Morel FMM, Rueter J, Anderson DM, Guillard R (1979) Aquil: a chemically defined phytoplankton culture medium for trace metal studies. J Phycol 15:135–141

Nimer NA, Brownlee C, Merrett MJ (1994) Carbon dioxide availability, intracellular pH and growth rate of the coccolithophore *Emiliania huxleyi.* Mar Ecol Prog Ser 109:257–262

Pierangelini M, Stojkovic S, Orr PT, Beardall J (2014) Elevated CO_2 causes changes in the photosynthetic appara-

tus of a toxic cyanobacterium, *Cylindrospermopsis raciborskii*. J Plant Physiol 171:1091–1098

Ratti S, Giordano M, Morse D (2007) CO_2-concentrating mechanisms of the potentially toxic dinoflagellate *Protoceratium reticulatum* (Dinophyceae, Gonyaulacales). J Phycol 43:693–701

Raven J (1990) Sensing pH? Plant Cell Environ 13: 721–729

Raven JA (1997) CO_2-concentrating mechanisms: a direct role for thylakoid lumen acidification? Plant Cell Environ 20:147–154

Raven JA, Kübler J, Beardall J (2000) Put out the light, and then put out the light. J Mar Biol Assoc UK 80:1–25

Raven JA, Beardall J, Giordano M (2014) Energy costs of carbon dioxide concentrating mechanisms in aquatic organisms. Photosynth Res 121:111–124

Riebesell U, Fabry VJ, Hansson LM, Gattuso JP (2010) Guide to best practices for ocean acidification research and data reporting. The Royal Society, London

Ritchie RJ (2006) Consistent sets of spectrophotometric chlorophyll equations for acetone, methanol and ethanol solvents. Photosynth Res 89:27–41

Roy RN, Roy LN, Vogel KM, Porter-Moore C and others (1993) The dissociation constants of carbonic acid in seawater at salinities 5 to 45 and temperatures 0 to 45°C. Mar Chem 44:249–267

Sabine CL, Feely RA, Gruber N, Key RM and others (2004) The oceanic sink for anthropogenic CO_2. Science 305: 367–371

Sano Y, Williams SN (1996) Fluxes of mantle and subducted carbon along convergent plate boundaries. Geophys Res Lett 23:2749–2752

Shiraiwa Y (2003) Physiological regulation of carbon fixation in the photosynthesis and calcification of coccolithophorids. Comp Biochem Physiol B Biochem Mol Biol 136: 775–783

Smith FA, Raven JA (1979) Intracellular pH and its regulation. Annu Rev Plant Biol 30:289–311

Strickland JDH, Parsons TR (1968) A practical handbook of seawater analysis. Bull Fish Res Board Can 167:49–80

Suffrian K, Schulz KG, Gutowska M, Riebesell U, Bleich M (2011) Cellular pH measurements in *Emiliania huxleyi* reveal pronounced membrane proton permeability. New Phytol 190:595–608

Tortell PD, Rau GH, Morel FM (2000) Inorganic carbon acquisition in coastal Pacific phytoplankton communities. Limnol Oceanogr 45:1485–1500

Tsuji Y, Suzuki I, Shiraiwa Y (2009) Photosynthetic carbon assimilation in the coccolithophorid *Emiliania huxleyi* (Haptophyta): evidence for the predominant operation of the C3 cycle and the contribution of β-carboxylases to the active anaplerotic reaction. Plant Cell Physiol 50: 318–329

Wu YP, Gao KS, Riebesell U (2010) CO_2-induced seawater acidification affects physiological performance of the marine diatom *Phaeodactylum tricornutum*. Biogeosciences 7:3855–3878

Yang GY, Gao KS (2012) Physiological responses of the marine diatom *Thalassiosira pseudonana* to increased pCO_2 and seawater acidity. Mar Environ Res 79:142–151

Zou DH, Gao KS (2014) Temperature response of photosynthetic light- and carbon-use characteristics in the red seaweed *Gracilariopsis lemaneiformis* (Gracilariales, Rhodophyta). J Phycol 50:366–375

Editorial responsibility: Zoe Finkel, Sackville, New Brunswick, Canada

Submitted: June 23, 2016; Accepted: February 20, 2017
Proofs received from author(s): April 22, 2017